Reservoir characterization via time-lapse prestack seismic inversion

Susan Minkoff, Sandia National Labs, William Symes, Rice University, Steve Bryant, Joe Eaton, Mary Wheeler, University of Texas at Austin*

Summary

Differencing of time-dependent seismic monitor surveys requires that datasets are collected and processed consistently. Inconsistencies can result in data difference noise great enough to obscure any reservoir changes. Inversion applied to each dataset may account for some of these inconsistencies. As an example, if the shape, temporal location, or radiation pattern of the seismic energy source is not known exactly, data differencing would produce only noise. However, we have shown in previous work that both the source and reflectivity can be accurately recovered via inversion. In this paper we describe a synthetic experiment in which the reservoir contains only oil and water initially. A single production well induces a pore pressure drop and related saturation changes including the formation of a gas cap. This work provides a baseline (best-case) scenario for testing the effectiveness of applying inversion to seismic time-lapse data — we assume that the source is known. Prestack inversion recovers both the subtle increase in S-wave impedance and the larger decrease in the P-wave impedance at the well location in the reservoir.

Introduction

Traditional time-lapse seismic imaging theory states that in a active oil field, the rocks surrounding a reservoir are not changing substantially with time. The reservoir fluids, however, are. Therefore, by differencing seismic data sets collected over time, one should be able to gain an understanding of the complexities of the flow paths within a particular reservoir. Unfortunately, one's ability to see the subtle migration of fluids in a reservoir on the much coarser seismic scale relies heavily on the assumption that the experimental acquisition geometry, collection technology, and processing do not change from survey to survey (Lumley, 1995). This assumption will never strictly hold, and the chance of it remaining true diminishes with the length of time the field is under study. Because even very minor differences in data collection and processing can cause large changes in the seismic data difference cubes, we advocate an alternative: apply inversion directly to each time-dependent data set.

In this paper we describe a realistic synthetic time-lapse study in which a single production well produces both pressure and saturation changes in the reservoir which we quantify by Gassmann's formulas. We forward model and invert the associated seismic data at the start and end of the flow simulation time period and show inversion, with the correct source, does an excellent job of recovering the elastic reservoir rock property changes with time. With even a slightly incorrect source, data differencing produces only noise. However, inversion can be extremely effective in estimating source changes as well (Minkoff and Symes, 1997). In the remainder of the paper, we describe the three main theoretical components of a time-lapse experiment — flow simulation, seismic imaging, and the rock physics link between the two processes. We then describe the numerical experiment in detail.

Reservoir Simulation

For the fluid flow simulations, we used a black oil reservoir simulator from the University of Texas which models the flow of three fluid phases: oil, gas, and water. (For a complete description of the model, see Aziz and Settari (1979)). Assumptions for using the black oil model include that water and oil are immiscible and do not change phase. Gas is soluble in oil, but not in water, and the fluids are assumed to be at constant temperature throughout the reservoir.

Given that N_i is the stock tank volume of component i ($i = o, g, w$) per unit pore volume, $\phi(P_w)$ is porosity, R_o is the stock tank volume of gas dissolved in a stock tank volume of oil, and q_i = the total stock tank rate of injection of phase i, the mass balance equations are

$$\begin{aligned} &\tfrac{\partial}{\partial t}(\phi N_g) = \nabla \cdot (U_g + R_o U_o) + q_g \\ &\tfrac{\partial}{\partial t}(\phi N_i) = \nabla \cdot U_i + q_i \qquad\qquad i = oil, water \end{aligned} \tag{1}$$

Darcy's Law gives the mass velocity U of phase i:

$$U_i = \frac{K k_{ri}}{B_i \mu_i} \cdot (\nabla P_i - \rho_i g \nabla D)\,. \tag{2}$$

Here, K is the diagonal permeability tensor, and k_{ri} is the relative permeability of phase i. B_i is the formation volume factor for phase i. P_i is pressure, and ρ_i is density. Gravity has magnitude g, and D is depth.

Finally, capillary pressure, fluid phase densities, and saturations, S_i, are determined by the following equations:

$$\begin{array}{ll} P_{cow}(S_w) = P_o - P_w & P_{cgo}(S_g) = P_g - P_o \\ S_o = B_o N_o & \rho_o = (\rho_{os} + R_{so}\rho_{gs})/B_o \\ S_g = B_g(N_g - R_{so}N_o) & \rho_g = \rho_{gs}/B_g \\ S_w = B_w N_w & \rho_w = \rho_{ws}/B_w \\ S_g + S_o + S_w = 1 & \end{array} \tag{3}$$

The solution gas ratio, $R_{so}(P_w)$, gives the mass transfer between the oil and gas phases as a function of pressure. The stock tank density of component i is ρ_{is}, and μ_i is viscosity.

The black oil model code is a fully implicit, 3-D, parallel subset of a more detailed compositional simulator. (For a description of the parallel framework, see Parashar et al. (1997)). The flow domain is parceled to different processors using domain decomposition, and the flow equations are discretized using an extended mixed finite element method which maintains local conservation of mass. The poorly conditioned nonlinear system is solved via a preconditioned, parallel, GMRES iterative method (see Edwards (1998)).

Gassmann's Equations

We convert the time-dependent reservoir pressures and saturations resulting from the flow simulation into elastic rock parameter changes (see Lumley (1995) for more details). These saturated rock parameters are fed directly into the seismic modeling code. Gassmann's equations provide a way to compute the effective bulk and shear moduli (K and μ respectively) of reservoir rock saturated with a given composition of pore fluids from the elastic moduli of the dry rock. These equations are

$$\mu_{sat} = \mu_{dry} \tag{4}$$

$$\frac{K_{sat}}{K_{solid} - K_{sat}} = \frac{K_{dry}}{K_{solid} - K_{dry}} + \frac{K_{fluid}}{\phi(K_{solid} - K_{fluid})} \tag{5}$$

They require knowledge of the effective bulk modulus of the pore fluid K_{fluid} (a function of both pressure and saturation), the porosity ϕ, the bulk and shear moduli of the dry rock with empty pores K_{dry}, μ_{dry} (functions of pressure), and the bulk modulus of the mineral material making up the rock K_{solid}.

We calculate the fluid phase bulk modulus and density by

$$\frac{1}{K_{fluid}} = \frac{S_w}{K_w} + \frac{S_o}{K_o} + \frac{S_g}{K_g} \tag{6}$$

$$\rho_{fluid} = S_w\rho_w + S_o\rho_o + S_g\rho_g. \tag{7}$$

From Gassmann's equations and relationships between elastic parameters we can determine the density ρ, compressional wave velocity V_p and shear wave velocity V_s at a given fluid saturation and pressure via

$$\rho_{sat} = (1-\phi)\rho_{solid} + \phi\rho_{fluid} \tag{8}$$

$$Vp_{sat} = \sqrt{\frac{K_{sat} + \frac{4}{3}\mu_{sat}}{\rho_{sat}}} \tag{9}$$

$$Vs_{sat} = \sqrt{\frac{\mu_{sat}}{\rho_{sat}}} \tag{10}$$

Seismic Modeling and Inversion

For forward modeling and inversion of the seismic data, we used The Rice Inversion Project's layered elastic linearized inversion code. The code was written using the C++ **H**ilbert **C**lass **L**ibrary (Gockenbach and Symes, 1996) and models 3-dimensional elastic wave propagation with the following assumptions. First, the earth is assumed to be layered, i.e., the elastic parameters are functions of depth only: $V_P(z)$, $V_S(z)$, $\rho(z)$. Second, we do not model multiple reflections. Therefore, we can linearize the parameters in the wave equation (for example, $\rho(z) = \rho_0(z) + \delta\rho(z)$). Finally, the source is assumed "high frequency", and we apply geometric optics approximations. These assumptions result in the convolutional model for the seismogram:

$$d^{pred}(t,h) = f(t,h) * \tilde{r}(t,h) \tag{11}$$

where d^{pred} is the predicted seismic data, f the source wavelet, h is offset, and t is time. The reflectivity: $\tilde{r}(t,h) \approx (A_P(z,h)r_P(z) + A_S(z,h)r_S(z) + A_D(z,h)r_D(z))_{z=Z(t,h)}$ where $Z(t,h)$ is the depth corresponding to two way time t at half offset h, A_P, A_S, and A_D are geometrical amplitude factors, and P-wave velocity, S-wave velocity, and density reflectivities are $r_P = \delta V_P/V_P$, $r_S = \delta V_S/V_S$, and $r_d = \delta\rho/\rho$.

We use an iterative conjugate gradient algorithm to solve the discrete linear system resulting from the inversion. The objective function contains two terms. Minimize:

$$J_{OLS}[r] = \frac{1}{2}\{\|d^{pred}[r] - d^{obs}\|^2 + \lambda^2\|W[r]\|^2\}.$$

The first term minimizes the data misfit (output least squares inversion) while the second term reduces the ill-conditioning of the system.

A Numerical Example

The time-lapse example described in this paper is based on the Stratton Field of South Texas. A subset of the field data (both stacked seismic and well logs) is publicly available through the Bureau of Economic Geology at the University of Texas. Stratton contains very thin reservoirs from the middle Frio Formation. (For detailed information on Stratton see the report by Levey et al. (1993).) The experiment we describe here is heavily based on properties of Frio sandstones and well logs included with the Stratton data. The stacked seismic data was not appropriate for prestack inversion.

To construct an initial set of elastic parameters for the total seismic depth of interest (4600-6900 ft), we started from a measured density log. We used Gardner's relation to estimate P-wave velocity from density (Castagna et al., 1993, p. 142). We then estimated a reasonable shear wave velocity from experimental relationships between P and S-wave velocities for Frio sandstones (Castagna et al., 1985, p. 574).

We decomposed the elastic parameters into low frequency (background) and high frequency (reflectivity) components suitable for the linearized modeling and inversion codes. This process resulted in modeled seismic data which placed the reflectors at the correct depths according to the Stratton Report.

We focused the time-lapse study on one reservoir located just above 1.6 s depth (approximately 6400 ft). Because of 1/4-wavelength limits on seismic resolution, we were forced to change the dimensions of the reservoir to be thicker in the depth direction. The reservoir porosity and permeability were chosen to be 20% and 35 md respectively in the top of the reservoir and 30% and 350 md in the lower half of the reservoir. These values fall into the measured porosity and permeability range for this reservoir.

The reservoir dimensions for the flow simulation are 1000x1000x66 ft. We assumed that the reservoir contains only oil and water initially. The pressure at the top of the reservoir is 3000 psi at the start of flow simulation, and the initial water saturation is 18%. During flow simulation, the reservoir undergoes a primary depletion mechanism consisting of a single production well located in the center of the flow domain $(x, y, z) = (550, 550, z)$ completed in the bottom half of the reservoir. Figure 1 show the oil saturation after 70 days flow simulation. After 15 days of flow simulation, the pore pressure has dropped to 2000 psi (the assumed bubble point pressure for the reservoir oil). The pore pressure remains close to constant from 15 days on. However, the saturation changes are significant after 15 days flow simulation due to the formation of a gas cap.

We will use the flow simulation saturation and pressure output and Gassmann's equations to predict the changes in the elastic parameters of the saturated reservoir rocks (at the well location). Gassmann's equations require knowledge of the solid rock bulk and shear moduli. These were estimated by calculating the solid rock velocities and density for zero-porosity Frio sandstones from Castagna et al., (1985, p. 573)

$$V_p(km/s) = 5.81 - 2.21 V_{cl} \quad (12)$$

$$V_s(km/s) = 3.89 - 2.04 V_{cl} \quad (13)$$

and then converting from Vp_{solid}, Vs_{solid}, and ρ_{solid} to K_{solid}, μ_{solid}. Here V_{cl} is the volume of clay (estimated to be 10% from the Stratton Report), and density measurements give that $\rho_{solid} = 2.65 g/cm^3$.

The fluid phase densities are determined from the mass-conservative reservoir simulator output and Equations (3). The fluid phase bulk modulus is calculated from Equation (6), where we assume that the bulk moduli of oil and water are $K_{oil} = 1020$ MPa and $K_{water} = 2089$ MPa. To calculate the adiabatic bulk modulus of gas we follow Lumley (1995, pp. 45–46) assuming a modified ideal gas law (for non-atmospheric reservoir pressures and temperatures).

Lastly, we need the dry rock bulk and shear moduli, K_{dry} and μ_{dry}, as a function of changing pressure. Castagna et al., (1993, p. 145) give an empirical relationship for calculating the effect of pressure on 100% brine-saturated Frio sandstone:

$$V_p = 5.77 - 6.94\phi - 1.73\sqrt{V_{cl}} + .446(P - e^{-16.7P}) \quad (14)$$

$$V_s = 3.70 - 4.94\phi - 1.57\sqrt{V_{cl}} + .361(P - e^{-16.7P}) \quad (15)$$

P is differential pressure (in kbars), and we assume a confining pressure of 6000 psi in the reservoir rock. The dry rock properties are determined from the brine-saturated moduli according to Castagna et al., (1993, p. 153).

From the solid rock bulk modulus, shear modulus, and density, the dry rock bulk and shear moduli, and the fluid bulk modulus and density, we apply Gassmann's equations (4, 5) to determine the saturated rock bulk and shear moduli at reservoir pressure for 1 day and 70 days flow simulation. The saturated rock bulk modulus changes with time are shown in Figure 2. Equations (8, 9, 10) give the saturated rock density and velocities.

Gassmann predictions show that the pore pressure drop (differential pressure increase) in the reservoir causes an increase in both P- and S-wave velocities. The formation of the gas cap causes a large decrease in density of the fluids and of the saturated rock. The P-wave velocity increase due to the differential pressure increase is offset by the decrease in saturated rock bulk modulus. The net result is a slight increase in V_p in the top of the reservoir and a slight decrease in the bottom. The top of the reservoir sees a bigger density decrease when the gas cap forms. Shear wave velocity is not affected by fluid saturations, but it increases due to the pressure increase.

Using Gassmann's predictions for the elastic parameters in the reservoir interval (6433–6499 ft), we forward model the seismic data over the whole depth interval (4610–6900 ft) at 1 day and 70 days. The resulting modeled data (which includes 11 reservoirs total) is inverted for elastic parameter reflectivities. Although elastic inversion is ill-posed, the results are encouraging. According to Gassmann's formulas, in the reservoir interval, the P-wave impedance decreases and the S-wave impedance increases slightly. The inversion captures both changes quite accurately. The P-wave impedance reflectivity from Gassmann's predictions and the inversion are shown in Figure 3. Outside of the reservoir interval, there is no change in either the inversion-estimated or Gassmann-predicted reflectivities.

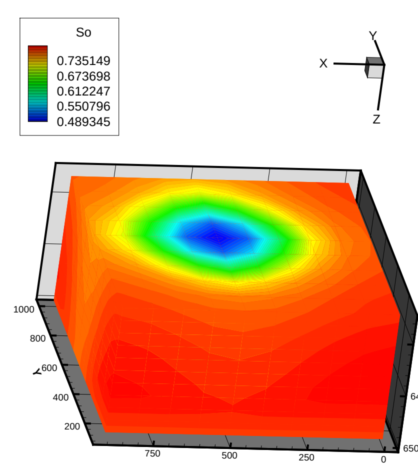

Fig. 1: Oil saturation after 70 days flow simulation.

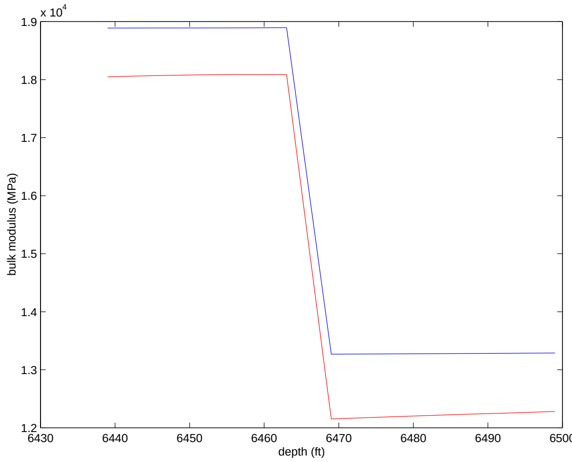

Fig. 2: The saturated rock bulk modulus at the well location from Gassmann's equations. Blue is at 1 day, red is at 70 days flow simulation.

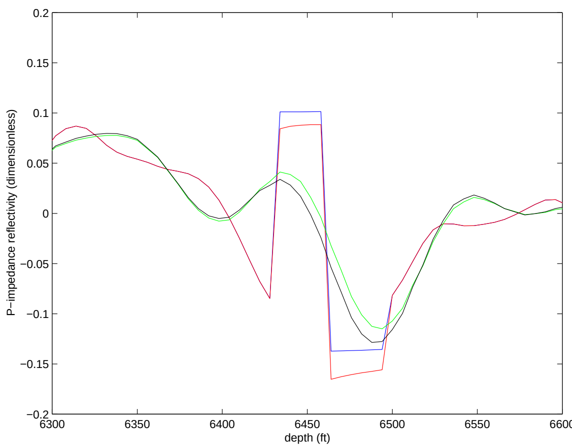

Fig. 3: P-impedance reflectivity in the reservoir interval (6433–6499 ft) from Gassmann's predictions (blue=1 day flow simulation; red=70 days flow simulation) and inversion (green=1 day flow simulation; black= 70 days).

Conclusions

Using a 3-phase black oil reservoir simulator, Gassmann's equations, and prestack seismic forward modeling and inversion, we have constructed a realistic synthetic time-lapse study based on the Stratton Field of South Texas. During the 70 days of flow simulation, the production well induces a pore pressure drop of more than 1000 psi in the reservoir, and an oil saturation decrease of nearly 50% in the vicinity of the well from primary depletion and the formation of a gas cap. We use Gassmann's predictions of the saturated rock bulk and shear moduli at 1 and 70 days for forward modeling and inversion. P- and S-wave impedances resulting from inversion closely match Gassmann's predictions in the reservoir interval. This experiment gives us a basis for the next step — including source inversion in the analysis of time-lapse data.

Acknowledgements

Susan Minkoff is supported by the U.S. Dept. of Energy under Contract DE-AC04-94AL85000, and by DOE's MICS Office. Sandia is a multiprogram laboratory operated by Sandia Corporation, a Lockheed Martin Company. William Symes thanks the sponsors of The Rice Inversion Project and NSF (grant #DMS 9627355) for their support. Mary Wheeler thanks the DOE (grant # 951522401) and the sponsors of the Industrial Affiliates Program at the Center for Subsurface Modeling.

References

Aziz, K., and Settari, A., 1979, Petroleum reservoir simulation: Applied Science Publishers Ltd., London.

Castagna, J., Batzle, M., and Eastwood, R., 1985, Relationships between compressional-wave and shear-wave velocities in clastic silicate rocks: Geophysics, **50**, 571–581.

Castagna, J., Batzle, M., and Kan, T., 1993, Rock physics — the link between rock properties and AVO response *in* Castagna, J., and Backus, M., Eds., Offset-Dependent Reflectivity: Theory and Practice of AVO Analysis:: SEG, 135–171.

Edwards, H., A parallel mulilevel-preconditioned GMRES solver for multiphase flow models in the implicit parallel accurate reservoir simulator (IPARS):, TICAM Report 98-04, University of Texas, Austin, TX, 1998.

Gockenbach, M., and Symes, W., 1996, The Hilbert Class Library: a library of abstract C++ classes for optimization and inversion:: Computers and Mathematics with Applications, **32**, no. 6.

Levey, R., Hardage, B., Langford, R., Scott, A., Finley, R., Sippel, M., Collins, R., Vidal, J., Howard, W., Ballard, J., J.D.Grigsby, and Kerr, D., Secondary natural gas recovery: targeted technology applications for infield reserve growth in fluvial reservoirs, Stratton field, South Texas:, Topical Report GRI-93/0187, Gas Research Institute, Chicago, IL, 1993.

Lumley, D., 1995, Seismic time-lapse monitoring of subsurface fluid flow: Ph.D. thesis, Department of Geophysics, Stanford University, Stanford, CA.

Minkoff, S., and Symes, W., 1997, Full waveform inversion of marine reflection data in the plane-wave domain: Geophysics, **62**, no. 2, 540–553.

Parashar, M., Pope, G., Wang, K., Wang, P., and Wheeler, J., 1997, A new generation EOS compositional reservoir simulator: Part II - framework and multiprocessing: Reservoir Simulation Symposium, Soc. Pet. Eng., Expanded Abstracts # 37977.